applied sciences

MDPI

Review

Disappearance of Mountain Glaciers in East Asian Monsoon Region since Onset of the Last Glacial Period

Rui Liu [1], Shuying Zang [1,*], Lin Zhao [2], Chunlei Wang [3], Boxiong Zhang [1] and Xiaodong Wu [4]

[1] Heilongjiang Province Key Laboratory of Geographical Environment Monitoring and Spatial Information Service in Cold Regions, Harbin Normal University, Harbin 150025, China
[2] School of Geographical Sciences, Nanjing University of Information Science and Technology, Nanjing 210044, China
[3] College of Integration Science, Yanbian University, Yanji 133002, China
[4] Cryosphere Research Station on the Qinghai–Tibet Plateau, State Key Laboratory of Cryospheric Science, Northwest Institute of Eco-Environment and Resources, Chinese Academy of Sciences, Lanzhou 730000, China
* Correspondence: zsy6311@hrbnu.edu.cn

Abstract: Discussing the development and shrinkage process of glaciers is of great significance for the in–depth comprehension of regional environmental evolution and predicting global changes. However, there is little understanding of the developmental and retreat processes of mountain glaciers during the Late Quaternary (150 ka) in the East Asian Monsoon region. Using the latest chronological glacial data from eastern China, Taiwan, the Russian Far East, and the Japanese islands of Hokkaido and Honshu, which are all regions impacted by the East Asian Monsoon, we screened reliable glacial age data. This study compiled and compared the age sequences of the different mountain glaciations (dating techniques included optically–stimulated luminescence (OSL), thermoluminescence (TL), electron spin resonance (ESR), U–series (U), cosmogenic nuclides (^{10}Be/CRN), carbon–14 (^{14}C) and potassium–argon (K–Ar), etc.). Based on the evolutionary features of the glaciations in these mountains, by comparison with the marine isotope stage (MIS) environment, the influence of monsoonal circulation patterns on the regional development of glaciers was analyzed. This study determined that Japanese mountain glacial stages since 150 ka are the most complete in the East Asian Monsoon region, having developed during MIS 6–1. Taiwanese mountain glaciers developed during MIS 4–1, but glacial stages in continental East Asia were relatively short, with glaciers first developing only during MIS 3b–1. The reason for this this phenomenon is that the tectonic uplift in different subregions was significantly different; on the other hand, it is also related to the difference of precipitation between land and sea in monsoon climate. By comparing the glacial glaciations in the East Asian Monsoon region with western China, we found that there were significant differences between the extent, onset time, and length of glacial periods. Since the Last Glacial Period, precipitation levels have become transitional and concentrated during the summer months, and temperatures have been continuously changing as a result of the many periodic changes in the East Asian Monsoon. From the Early Last Glacial Period (MIS 4) to the Middle Last Glacial Period (MIS 3b) to the Last Glacial Period (MIS 2/LGM–YD), climatic conditions increasingly restricted the development of glaciers; the regional environment continued to warm until glaciers completely disappeared during the Late Holocene.

Keywords: East Asian Monsoon; Last Glacial Period; monsoon circulations; mountain glaciation sequences

check for updates

Citation: Liu, R.; Zang, S.; Zhao, L.; Wang, C.; Zhang, B.; Wu, X. Disappearance of Mountain Glaciers in East Asian Monsoon Region since Onset of the Last Glacial Period. *Appl. Sci.* **2023**, *13*, 1678. https://doi.org/10.3390/app13031678

Academic Editor: Harry D. Kambezidis

Received: 10 December 2022
Revised: 25 January 2023
Accepted: 26 January 2023
Published: 28 January 2023

Copyright: © 2023 by the authors. Licensee MDPI, Basel, Switzerland. This article is an open access article distributed under the terms and conditions of the Creative Commons Attribution (CC BY) license (https://creativecommons.org/licenses/by/4.0/).

1. Introduction

East Asia is located in the western Pacific Ocean region, in the Eurasian hinterland. Affected by a strong sea–land thermal difference and the high–altitude Tibetan Plateau (TP), it provides a heat and water vapor transmission channel between Eurasia and the

Northwest Pacific. It is an important part of the global climate system [1]. Any changes in the East Asian Monsoon (EAM) can affect the economic and living conditions of two–thirds of the world's population. Understanding how the EAM climate can change is therefore of huge scientific and societal importance [2]. The modern monsoon system is characterized by strong seasonal variability. During the winter, when a principally northwesterly wind blows, the EAM region is very cold and dry; in the summer, the region is warm and humid [3]. The hot airmass transmitted to the EAM region by the southeasterly wind that blows from the Pacific Ocean dominates the summer months, when precipitation (P) levels are at their highest [4]. The EAM circulation has undergone many periodic changes since the Last Glacial Period (LGP). The alternation of the East Asian Summer Monsoon (EASM) and the East Asian Winter Monsoon (EAWM) affects temperatures (T) and P throughout the region [5–7].

Glaciers are highly sensitive to regional environmental changes. As such, they can accurately reflect long–term environmental change. Glacial proxies therefore have an irreplaceable role in delineating any changes in the regional climate and environment [8,9]. The potential correlation between glacial development (advance/stasis/retreat) and environmental change offers a new theoretical perspective, i.e., that Late Quaternary (150 ka) glaciers in the middle and low latitudes of East Asia may have resulted from the coupling of a particular region's climate and geomorphology [10–12]. It has been suggested that the Late Quaternary glacial period in the EAM region started late, in the Early LGP at the earliest [13]. Li [14] concluded that the coastal areas of East Asia approached, or reached, the equilibrium line altitude (ELA) for the development of glacial ice during the LGP, as a result of strong tectonic movement. On the other hand, other studies have maintained that, in response to the EAM climate, mountain glacier development (advance/stasis/retreat) depended more on P and T and exhibited some characteristics typical of marine glaciers [15–17]. Marine glaciers are heavily dependent on the supply of P and T, especially during the winter months, when falls of rain or snow can aid the development of glacial ice [18–21]. Shi [22] pointed out that the ELA in the EAM region during the Last Glacial Maximum (LGM) was more than 10 degrees of latitude further south than for areas of the same altitude in central Asia; the mountain paleo–ELA (ΔELA) for mountains in the EAM region was >500 m lower. Zhang et al. [23] stated that the ELA in the EAM region is now higher than the mountains in that region, explaining why modern glaciers cannot develop. Su et al. [24] proposed differences in glacial development patterns between the East Asian Intracontinental and the EAM regions. After all, scholars have recognized the climate and environmental particularity of glacier development in the study area; the key point of the study is the earliest time and the driving factors of glacier development. There remains a paucity of research into the evolutionary features of the glacial stages in the mountain ranges of this particular climatic region. Furthermore, the specific relationship between different glacial stages and the monsoon environment has yet to be fully explored.

This study has attempted to clarify the developmental characteristics of different glacial stages in the mountains of the EAM region and discover the principal reasons for the region's deglaciation. The resulting mountain glacial history of the EAM region has important scientific significance for future detailed discussions about the mechanisms affecting the regional advance and retreat of glaciers, as well as the EAM region's environment during different glacial stages, in relation to global climate change.

2. Study Area Description

The study area is located in East Asia, along the northwestern coast of the Pacific Ocean. The general orientation of the EAM region extends east of the Asian continent at 105 °E to the East Asian island archipelagos and the Pacific Ocean, with the area with the strongest monsoonal influence being south of 58 °N (Figure 1). At present, P in the studied monsoonal regions of East Asia comes mainly from the EASM. Both the accumulation and the ablation of glacial ice are concentrated in the summer, but there are no modern glaciers

within the region. The study area does not include the area affected by both the EAM and the Indian summer monsoon (ISM) (Table 1).

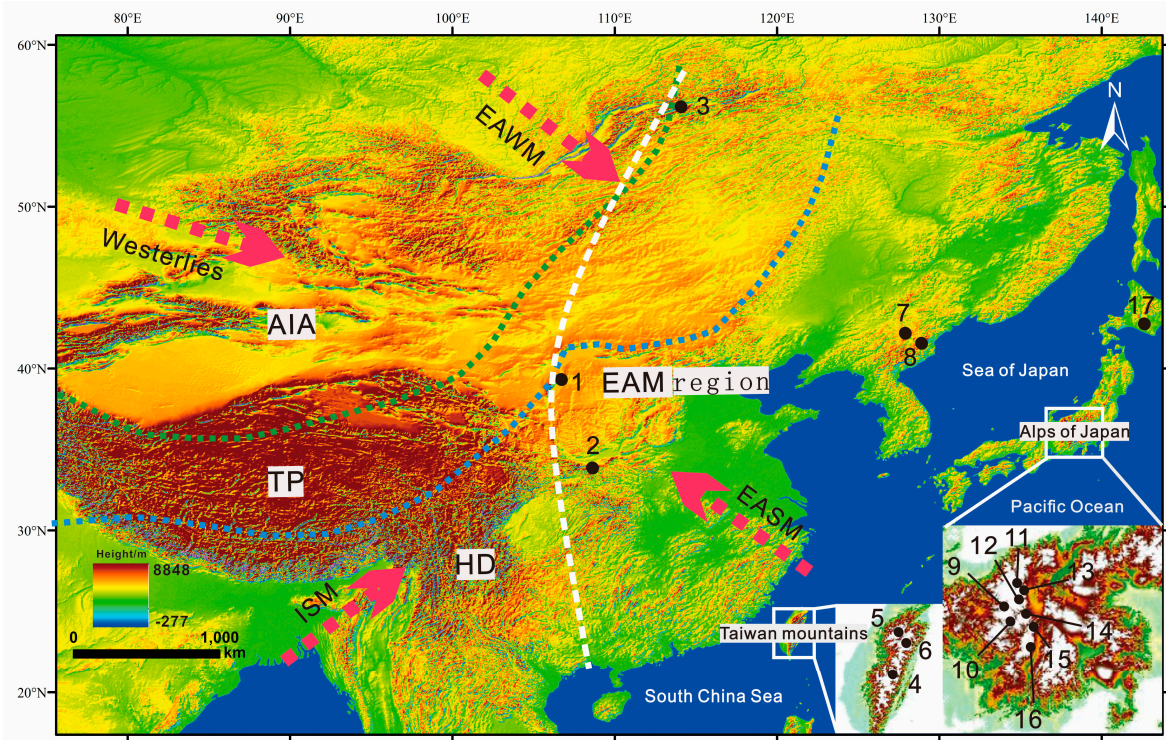


Figure 1. Location of the glaciated mountains in the study area DEM. Green dotted lines represent the present limits of monsoonal precipitation, blue dotted lines represent the LGP limits of monsoonal precipitation. East of white dotted lines represent the study area, lines reference from [22]. 1: Helan Mountains; 2: Mount Taibai; 3: Barguzinsky Range; 4: Mount Yusan; 5: Mount Shesan; 6: Mount Nanhuta; 7: Changbai Mountains; 8: Kaema Plateau; 9: Mount Kurobegoro; 10: Mount Yumiore; 11: Mount Shirouma; 12: Mount Suisho; 13: Mount Tateyama; 14: Mount Kashima–Yari; 15: Mount Hotaka; 16: Mount Kisokoma; 17: Hidaka Range.

Table 1. Physical geography of the study area.

Mountains	Latitude (°N)	Longitude (°E)	Elevation (m a.s.l.)	MAP [1] (mm)	MAT [2] (°C)	WS [3] (m a.s.l.)	References
Helan Mts	38.00 −39.30	105.11 −106.45	3556	430	−0.8	2901	[25]
Mt Taibai	33.40 −34.10	107.19 −107.58	3767	750	−2	1543	[26]
Changbai Mts	41.58 −42.06	127.54 −128.08	2691	1340	−7.3	2624	[27]
Kaema Plateau	42.11 −39.59	126.31 −129.34	2541	1500	−5.8	1500	[28]
Taiwan Mts	24.54 −22.15	120.48 −121.41	3952	2500	24	3054	[29]
Russian Far East Mts	48.47 −56.59	110.07 −138.29	2640	900	−13	1880	[30]
Hidaka Range	42.09 −43.02	142.37 −143.17	2052	1035	5.9	1701	[31]
Japan Alps	35.04 −37.06	137.37 −138.42	3775	1800	14.7	3355	[32]

([1] MAP: Mean annual precipitation, [2] MAT: Mean annual temperature, [3] WS: Weather station).

3. Methods and Datasets

3.1. Method Description

In this study, we compiled the regions affected by EMA circulation. Using the latest chronological glacial data from eastern China, Taiwan, the Russian Far East (RFE), and the Japanese islands of Hokkaido and Honshu, a total of 117 moraine ages from 16 different mountains or mountain ranges were obtained and merged into 29 groups of data (Table 2). It should be noted that widely disputed low–altitude mountain glaciers (<1800 m) were not included in this study. The dating methods included optically stimulated luminescence (OSL), thermoluminescence (TL), electron spin resonance (ESR), U–series (U), cosmogenic nuclides (^{10}Be/CRN), carbon–14 (^{14}C) and potassium–argon (K–Ar), etc. Before compiling the moraine relic data set, the geological composition of the relevant strata should be carefully checked. We ruled out the wrong geomorphological sampling ages of some non–moraine sediments, which ensured the reliability of glaciations. It should be noted that widely disputed low–altitude mountain glaciers (<1800 m) are not included in the study.

Table 2. Statistical of moraine ages in EAM region.

Mountains	Altitude (m)	Dating Method	Ages Range (ka) [1]	References
Helan	3556	OSL	1.7 ± 0.1–43.2 ± 4.0	[33]
		ESR	19 ± 2.1	[34]
Taibai	3767	^{10}Be	15.1 ± 1–18.6 ± 1.1	[26]
		ESR, OSL	24 2.74 ± 0.11–7.6 ± 0.2.7	[35]
		OSL	18.7 ± 1.1–25.8 ± 1.8	[36]
Changbai	2691	OSL	11.3 ± 1.2–20.0 ± 2.1	[37]
Yusan	3952	OSL	3.3 ± 1.1	[38]
Shesan	3886	TL	10.68 ± 0.84–44.25 ± 3.72	[39]
		OSL	55 ± 4	[38]
Nanhuta	3740	^{10}Be	3.3 ± 0.73–13.61 ± 1.45	[40]
		^{10}Be	10 ± 3–7 ± 1	[41]
Barguzinsky	2436	OSL	10 ± 1.3–34 ± 3.9	[42]
		K–Ar	40 ± 5	[43]
Hidaka	2052	U	112–115	[44]
		OSL	18–24	[45]
		^{14}C	25.15 ± 2.1	[46]
Kurobegoro	2840	^{10}Be	10.1 ± 1.1–13.9 ± 1.1	[47]
Yumiore	2592	^{10}Be	11 ± 1	[47]
Shirouma	2932	U	120–134	[44]
		^{14}C	25	[48]
Suisho	2986	^{10}Be	8.3 ± 0.7–10.4 ± 1.1	[47]
Tateyama	3015	^{10}Be	10–29	[49]
		^{14}C	50–52	
		OSL	60–75	[50]
Hotaka	3190	OSL	18–72	[51]
Kashima–Yari	3180	K–Ar	120–130	[52]
		^{14}C, CRN	16–78	[53]
Kisokoma	2956	K–Ar	25–75	[54]

([1] Quaternary chronologies: Quaternary, since 2650 ka (MIS98); Penultimate Glaciation, 360–135 ka (MIS106); Last Interglacial, 135−75 ka (MIS5); Early Last Glacial Period, 75−50 ka (MIS4); Middle Last Glacial Period, 45−32 ka (MIS3); Late Last Glacial Period, 32−10 ka (MIS2); Holocene, since 10 ka (MIS1)).

Based on the evolutionary features of the glaciations in these mountains, by comparison with marine isotope stage (MIS) environment, the influence of monsoonal circulation patterns on the regional development of glaciers was analyzed. The EAM record and changes in its monsoonal circulations were examined, and the proxy records (e.g., the insolation curve, cave stalagmite, ice core, sea sediment, loess mean grain size, and lake sediment) of multiple monsoon climate were compared and analyzed. We attempted to delineate the evolution of the EAM region's climatic environment and the impact that such an evolution may have had upon the development, i.e., the advance, stasis, or retreat, of glaciers within the region. Furthermore, the data was used to establish the potential reasons for the disappearance of regional glaciers in the EAM region during the Late Holocene. A comprehensive and in–depth understanding of the occurrence, onset times, extent and

environmental evolution of the EAM region's glaciers and glacial stages, as well as their dates, was established.

3.2. Spatiotemporal Distribution of Mountain Glacier Records in the EAM Region

3.2.1. Eastern China Mountains

- Helan Mountains

The Helan Mountains are located in northern China. There are clear traces of glaciation >2800 m above sea level (asl); two–stage cirques and geomorphic features typical of glaciation are distributed on both sides of the ridge. Using field investigations and comparisons between different OSL dating datasets, we confirmed that there were four glacial advances in the Helan Mountains, i.e., during the middle LGP (MIS 3b; 43.2 ± 4.0 ka), the LGM (19.3 ± 1.4 ka), the Younger Dryas event (YD) (12.0 ± 1.1 ka), and the Holocene glacial period (MIS 1; 3.4 ± 0.3 ka and 1.7 ± 0.1 ka) [33]. At present, there is no term for any corresponding glaciation sequences.

- Mount Taibai

Mount Taibai is the highest peak in eastern China. It is located in the Qinling Range, which is considered to represent the dividing line between the northern and southern China. Scientists have proposed highly divergent onset times and geomorphic distributions for Mount Taibai's Late Quaternary glaciers; there are also differing views on the subdivision of the Late Quaternary glacial period, whether that be into multiple glacial stages, four glacial stages, two glacial stages, or even two substages of one glacial period [55,56]. Rost [34] dated the inner moraine below the Sanqingchi Tarn in the upper reaches of the Heihe Valley to 19 ± 2.1 ka used ESR dating, corresponding to the Eryehai glacial stage of the LGM. Zhang et al. [37], Gu [35] and Liu et al. [36] used ESR, ^{10}Be, and OSL dating techniques, respectively, to determine the date of the moraines on Mount Taibai, and variously came up with dates of 22.1 ± 1.7–15.07 ± 0.92 Ka, corresponding to the Dayehai glacial stage of the LGM–LGP; dates of 7.6 ± 0.27 ka, 3.51 ± 0.16 ka and 2.74 ± 0.11 ka corresponded to the Baxiantai glacial stage of the Holocene glacial period (MIS 1), when the glacial retreat that had occurred after the LGM was temporarily reversed. The geomorphic properties of the three sets of lateral moraines in the Eryehai valley indicate that they are likely to be the products of different stages of the LGP. Indeed, it is possible that there may have been an earlier glacial stage (i.e., the Yuhuang stage, MIS 3b).

- Changbai Mountains

Baiyun Peak on the Chinese side of Lake Tianchi in the Changbai Mountains is the highest peak in northeastern China. Late Quaternary glacial geomorphic features are clearly preserved above 2000 m asl in the Changbai Mountains, showing evidence of multiple glaciations. However, the history of these glacial stages and their specific subdivision has remained unclear, principally due to erosion and volcanic activity that has affected the accurate dating of moraines. In recent years, using the OSL dated ages of moraines around the Baiyun Peak stratovolcanic crater and combining these findings with the relationship between glacial development and volcanic activity, two glacial stages in the Changbai Mountains have been determined, i.e., the Heifengkou glacial stage at 20.0 ± 2.1 ka during the LGM and the Qixiangzhan glacial stage at 11.3 ± 1.2 ka during the YD [37]. Earlier glaciations remain to be further investigated.

3.2.2. Taiwan Mountains

Whether or not there is any geomorphic evidence of Late Quaternary glaciation in Taiwan has been controversial due to the lack of chronological evidence [57]. However, it has been established that Late Quaternary glaciers in Taiwan were distributed in the high mountains of the island's eastern central sector. Using the geomorphic properties of these mountain glaciers, Taiwanese scientists have subdivided them into two categories: a "direct melt type" and a "retreat melt type" [58,59]. Cui et al. [39] used TL dating to date

glacial sediments from Mount Shesan in Taiwan, and divided them into the Shanzhuang glacial stage (corresponding to 55 ± 4 ka −44.25 ± 3.72 ka) during the early LGP (MIS 4), the Shuiyuan glacial stage (corresponding to 18.26 ± 1.52 ka) during the LGM, and the Shesan glacial stage (corresponding to the YD event during the LGP). Scholars used ^{10}Be and OSL dating techniques to measure glacial sediments and boulders on Mount Yusan, Mount Nanhuta, Mount Shesan, and other peaks, giving results that ranged between 55 ± 4 ka and 3.3 ± 1.1 ka [38–41]. These dating results supported previous subdivisions of the glaciation sequences of Taiwan's mountain ranges [39,60]. Zhu et al. [61] speculated that the large–scale, two–stage cirques evident on Mount Yusan may be older than the early LGP.

3.2.3. North Korea Kaema Plateau

The Kaema Plateau is located in south of the Changbai Mountains and can be considered an integral part of the eastern Changbai Mountains. There are many traces of glaciation on the main Kwanmo Peak and its surrounding mountains [62]. According to [63], 14 large and small cirque groups are distributed on the eastern and northern slopes of the Kaema Plateau above 1900 m asl; the ΔELA at the peak of the LGM on the Kaema Plateau was ~2000 m asl, ~300 m lower than for the Changbai Mountains proper. At present, there is no specific research available for glaciation ages in North Korea. However, considering the region's geomorphic features and combining this knowledge with data from the surrounding Changbai and Hidaka mountain ranges, we could speculate that the earliest onset time of the Late Quaternary glacial period is unlikely to be earlier than the middle LGP (MIS 3b).

3.2.4. RFE Mountains

The RFE is located in the subfrigid zone, where the climate is conducive to glacial development. Astakhov [64] showed that a large–scale ice sheet appeared during the LGP in Siberia, and that its onset time was significantly earlier than for other ice sheets in the Northern Hemisphere (e.g., the Novayazemlya ice sheet in central Siberia reached its maximum extent at 50−40 ka [65–67]). During the LGP, mountain glaciers developed extensively under the impact of the colder climate. There are traces of the LGP in the Sichote Range, the Yam–Alin Mountains and the Baygal Highlands in the western section of the Stanovoy Range, where the climate is dominated by the RFE East Monsoon System [14]. Russian scientists named a set of Zyryan glaciation sequences that correspond to the LGP in eastern Siberia; the early and middle stages constitute the Zyrianka glacial stage, whereas the late stage is the Sartan glacial stage [68]. Glaciations in the Barguzinsky Range in the Baygal Highlands have been chronologically dated to 39−34 ka for the middle LGP (MIS 3b), 22−18 ka for the LGM, and 13−10 ka for the YD [42]. Stauch et al. [69] speculated that in the middle LGP (>MIS 3b), ice input in the mountains was principally affected by ice sheet activity, and that the temperature gradually increased and glaciers gradually decreased after the warmer middle LGP stage (MIS 3c).

3.2.5. Japanese Mountains

The mountain glaciers in Japan are distributed in the Hidaka Range on Hokkaido, and the Alps on Honshu. The Japanese archipelago extends more than 3000 km from south to north, and the climate ranges from subtropical to cold–temperate. There are some differences in the geographical environment between Hokkaido and Honshu, and differently subdivided and named glaciation sequences have been adopted.

- The Hidaka Range on Hokkaido

The remains of paleoglaciers can be seen in the Hidaka Range in the southeast of Hokkaido Island, at an altitude of 1400–1500 m asl; a superimposed grouping of cirques is also traceable around Mount Tottabetsu and Mount Poroshiri. The Tottabetsu and Poroshiri glacial stages have therefore been named from two unconformable sets of moraines on these mountains [70]. Japanese scholars used volcanic ash sequences to reconstruct the

stratigraphy of the Hokkaido glacial stage; they named the Poroshiri glacial stage after a moraine near Lake Shikotsu dated to 40 ± 5 ka (MIS 3b). The widely–accepted Tottabetsu glacial stage corresponds to the late LGP (MIS 2) and LGM [43]. However, some scientists have speculated, from analyses of moraine morphology, that there may have been even earlier glacial advances in the Esaoman Mountains. The Esaoman glacial stage has been dated to 115−112 ka U–series methods [44]. In recent years, with more in–depth analyses of the Hokkaido glacial stage, scholars have obtained two chronological datasets corresponding to 25.15 ± 2.1–18 ka (LGM) using OSL and ^{14}C dating; they have not found any evidence of glaciation in the early LGP and Holocene glacial stage, confirming the delineation of the Tottabetsu glacial stage [45]. This differs from the mountain glaciers that developed on Honshu Island [71].

- The Japanese Alps on Honshu

The paleoglacial geomorphic landforms of the Japanese Alps in central Honshu are principally distributed in the alpine belt above 2900 m asl in the three mountain ranges of the Northern Alps, the Central Alps and the Southern Alps [72]. Using the latest dating methods, Japanese scientists delineated different glaciation sequences/glacial stages for the mountains in the Japanese Alps [47,73]: the Karasawa, the Iwato and the Yokoo glacial stages. These represent late LGP (MIS 2), middle LGP (MIS 3b) and early LGP (MIS 4) paleoglacial relics, respectively, found on Mount Hotaka, the highest peak in the Northern Japanese Alps. There were multiple glacial advances during the YD and the Holocene glacial stage (MIS 1); glacial development was more extensive in the middle LGP and the early LGP (MIS 3/4) than in the late LGP (MIS 2) and the LGM [51–54]. However, some scholars have put forward opposing views. They believe that the mountains altitude and sufficient water vapor in the atmosphere over Honshu Island could have promoted the development of glaciers during the Penultimate Glaciation (MIS 6), thereby defining the Otanihara and the Yoshiwara glacial stages on Mount Kashima–yari and Mount Shirouma [52], based on volcanic ash sequence and U–series dates of 134−120 ka measured on Mount Shirouma, in the Northern Japanese Alps [44,46].

4. Sequences Features of Mountain Glacier Evolution in the EAM Region

4.1. Glacial Stages

Existing chronologies show that, although glacial advances throughout the region's mountain ranges were approximately consistent with the cold events described above, the onset of the Penultimate Glaciation (MIS 6) marked the earliest of the glaciations during the period (Figure 2), consistent with the glaciation sequences determined by early researchers using relative geomorphology/stratigraphy methodologies [70,74]. However, glacial advances and retreats in different mountain ranges during the studied glacial stages are not entirely consistent in terms of onset and retreat times.

4.1.1. Penultimate Glaciation and Last Interglacial (MIS6−5)

Of the mountain ranges studied in relation to their potential Late Quaternary glaciation, the Honshu Mountains of Japan saw the earliest glaciation. Mount Kashima–yari and Mount Shirouma in the Honshu Alps (both >2900 m asl), as well as Mount Esaoman (1900 m asl) in the Hidaka Range on Hokkaido, all show morphological evidence of the Otanihara, Yoshiwara and Esaoman glacial stages, during MIS 6–5 (Figure 2) [44,75]. At this time, glaciers began to develop across the EAM region.

4.1.2. Early LGP (MIS 4)

After the onset of the LGP, glaciers advanced in the early LGP (MIS 4) on Mount Tateyama, Mount Kashima–yari, Mount Shirouma, Mount Hotaka in the Northern Japanese Alps on Honshu, and on Mount Kisokoma and almost all the mountains in the Central Alps. Other mountains in the Honshu Alps and the Hidaka range on Hokkaido have not provided any direct evidence of glacial advances at this time. On Mount Shesan in Taiwan, scientists have discovered relics of the Shanzhuang glacial stage during the late

MIS 4 (55 ± 4 ka), similar to the glacial stage identified in Japan. This is the earliest Late Quaternary glacial stage yet recorded in Taiwan territories (Figure 2). This would suggest that Mounts Nanhuta and Yusan on the island of Taiwan, both with similar altitudes, should also have experienced a glacial advance during the early LGP, although no traces of a glacial advance at this stage have been found in inland mountain ranges, pointing to a potentially unique glaciation in the mountains of the East Asia island archipelagos at this time [50].

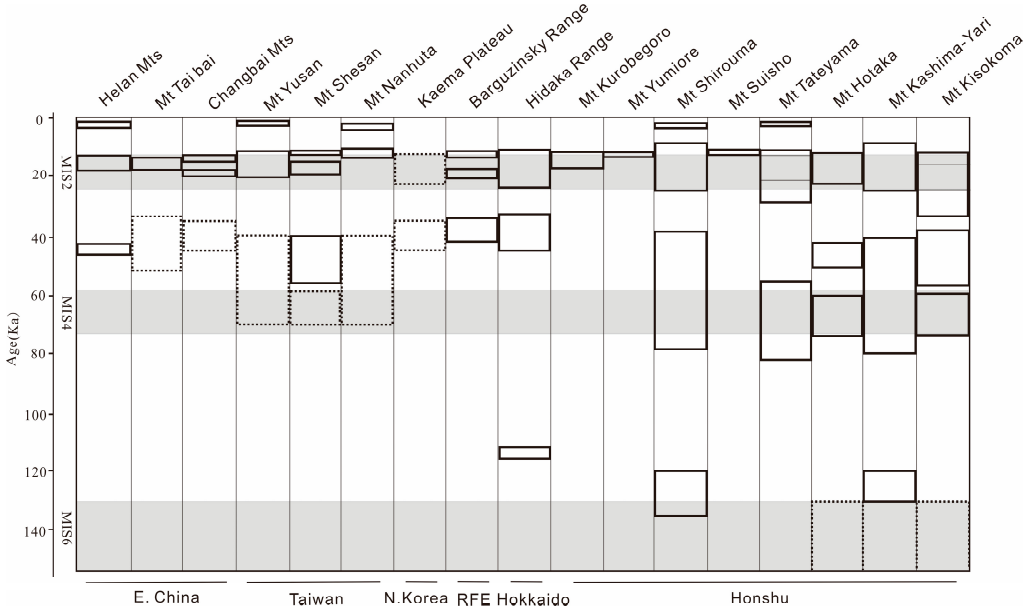


Figure 2. Comparison of the Late Quaternary glacial stages of different mountains in the EAM region. The solid lines represent the exact glacial stage, and the dotted lines represent the inferred glacial stage; The shaded areas represent the global cold period, and the unshaded areas represent the global warm period.

4.1.3. Middle LGP (MIS3b)

During the middle LGP glacial advance (MIS 3b), a date of 44.25 ± 3.72 ka was identified on Mount Shesan in Taiwan; the MIS 3b stage was dated to 43.2 ± 4.0 ka using analyses of glacial relics found in the Helan Mountains. Although the MIS 3b stage has not been identified on Mount Taibai, a peak of similar altitude to the south of the Helan Mountains, scientists have suggested that Mount Taibai would have experienced the Yuhuang glacial stage (MIS 3b), based on the area's glacial geomorphic relationship with neighboring mountains [26]. No MIS 3b traces have been found in the Changbai Mountains in northeastern China, although such a stage is believed to have occurred on the Korean Peninsula. A glacial stage corresponding to 39−34 ka has been identified in the Barguzinsky Range in the RFE and has been taken to signify the earliest onset time of the Late Quaternary glacial period in the RFE. There are many MIS 3b traces discernible in the Hidaka Range on Hokkaido; the glacial advance of the Poroshiri glacial stage is easily identifiable, but a similar glacial advance in the mountainous areas of Honshu Island is less clear. The Nakagosho II glacial stage identified on Mount Kisokoma was dated to 39−37 ka; the Ichinomata and Iwato glacial stages on Mount Kashima–Yari and Mount Shirouma, respectively, started at ~80 ka during the early LGP (MIS 4) and disappeared at ~40 ka and ~38 ka, respectively. This stage could be regarded as correspondent with the middle LGP (MIS 3b), glacial advances during the middle LGP (MIS 3b) have not been identified in other mountainous areas of Honshu [76] (Figure 2). At this time, the cooling time was relatively sudden, meaning that not all mountain ranges responded similarly, so the effect and scale of any cooling were not as strong as those experienced during the early LGP (MIS 4).

4.1.4. Late LGP (MIS 2)

During the late LGP (MIS 2/LGM), almost all the mountains in the EAM region responded to such a cooling of the climate: the Taibai glacial stage in the Helan Mountains and on Mount Taibai in eastern China, the Heifengkou glacial stage in the Changbai Mountains [33,35,39], and the Shuiyuan glacial stage in Taiwan [39], all indicate the existence of glacial advances in eastern China at this time. The Barguzinsky Range in the RFE shows evidence of a glacial stage at 22−18 ka [42]. Records of a glacial advance during this time can also be identified as the Tottabetsu glacial stage in the Hidaka Range on Hokkaido [45,46], the Tateyama glacial stage on Mount Tateyama on Honshu, the Yarisawa glacial stage on Mount Yarisawa, the Akakurasawa glacial stage on Mount Shirouma, the Karasawa glacial stage on Mount Hotaka, and the Nakagoshol glacial stage on Mount Kisokoma [48,49,51,53,54]. This would suggest that at least the majority of the EAM region experienced a general cooling at this time, consistent with the globally cooling climate. Many glaciations in mountains within the EAM region have also been identified as having taken place during the late LGP (YD), such as during the Dayehai glacial stage on Mount Taibai and in the Helan Mountains in eastern China, the Qixiangzhan glacial stage in the Changbai Mountains, and the Shesan glacial stage on Mount Shesan in Taiwan [26,33,37,39,40]. Almost all the mountains in the Barguzinsky Range in the RFE [42,47,49], as well as on the Japanese island of Honshu, show clear evidence of glaciations at this time (Figure 2), showing the regional consistency of this cooling event.

4.1.5. Holocene (MIS1)

Only a few high mountains in the EAM region show evidence of glacial advances during the Holocenes Neoglacial stage (MS 1), such as on Mount Yusan (dated to 3.3 ± 1.1 ka) and Mount Nanhuta (dated to 3.30 ± 0.73 ka) on Taiwan, in the Helan Mountains (dated to 3.4 ± 0.3 ka and 1.7 ± 0.1 ka), on Mount Taibai (dated to 7.6 ± 0.27 ka, 3.51 ± 0.16 ka and 2.74 ± 0.11 ka) and on Mount Suisho on Honshu (dated to 8.3 ± 0.7 ka) [33,35,38,40,47]. Therefore, it can be found that the glacial retreats of Helan Mountains at the latest in the EAM region (Figure 2).

4.2. Overall Changes of Glaciations

Of the whole EAM region, it is therefore apparent that the Late Quaternary glacial period was the most complete, and lasted the longest in the Japanese mountains. Of the mountains in eastern Chinese territories, the Late Quaternary glacial period experienced in the mountains of Taiwan was the most similar to that of Japan, i.e., the Late Quaternary glacial period lasted longer overall and was more complete. Several stages of glacial development are evident, from the Penultimate Glaciation and Last Interglacial (MIS 6−5), the early LGP (MIS 4), the middle LGP (MIS 3b), the late LGP (MIS 2/LGM) and the Last Glacial (YD) and the Holocene glacial stage (MIS 1) (Figure 2). The newly discovered glacial advance on Mount Nanhuta dated to 3.3 ± 1.1 ka during the Neoglacial stage shows that glaciers retreated relatively late in the mountains of Taiwan, consistent with the mountains of Japan, reflecting the particularity of these island archipelago mountain ranges. On the East Asian continent, glaciation sequences in the mountains there appear relatively short in duration. The Helan Mountains, which experienced the longest glaciation, experienced glacial advances during the middle LGP (MIS 3b), LGM, YD, and Holocene (MIS 1); 1.7 ± 0.1 ka also represents the latest record of a glacier melting on the East Asian continent. This corresponds to the late LGP glacial development experienced on Honshu at the same latitude in the east, although the Helan Mountains are nearly 500 m higher than the Japanese mountains affected. Interestingly, no glaciers developed on the eastern slopes of Mount Taibai and in the Changbai Mountains at this time. We could therefore speculate that the onset of the Late Quaternary glacial period on the Korean Peninsula was no earlier than the middle LGP (MIS 3b). In contrast, a middle LGP (MIS 3b) glaciation onset time in the higher–latitude mountains of the RFE is equivalent to the maximum extent of the Siberian ice sheet, with other glacial advances during the late LGP (MIS 2), the LGM, and

the Holocene glacial stage (MIS 1). The Former Soviet Union scholar Kind [77] believed that the glaciation experienced during the early Zyryan glacial stage in the early and middle LGP and was greater than that of the Sartan glacial stage during the late LGP. However, as a general rule, all mountain ranges influenced by the EAM have experienced gradually decreasing glaciations since the LGP (Figure 3).

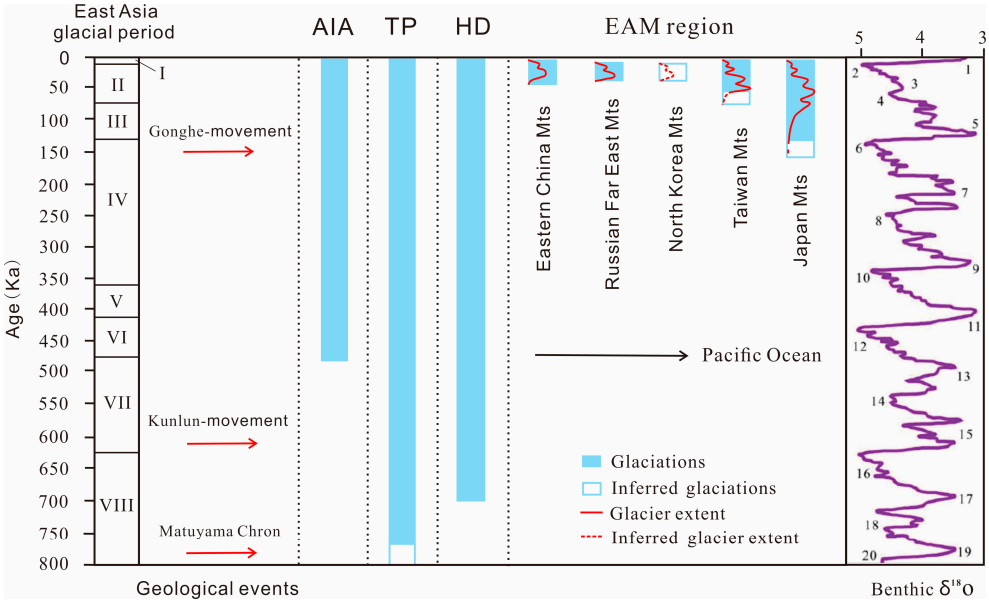


Figure 3. Comparison of mountains glacial period between EAM region and adjacent areas. Data reference from [9,13,78]. Benthic $\delta^{18}O$ curve reference from [79], numbers represent the marine isotope stages. I: Holocene; II: Last Glacial Period; III: Last Interglacial; IV: Penultimate Glaciation; V: Penultimate Interglacial; VI: Zhonglianggan Glaciation; VII: Great Interglacial; VIII: Wangkun Glaciation. AIA: Asia Inland area; TP: Tibet Plateau; HD: Hengduan Mountains, see Figure 1 for geographical location.

5. Discussion

5.1. Analysis of the Reliability of the Glacial Chronology of the EAM Region

Moraines are direct products of glacial events. The accumulation age of a moraine reflects the time of the glacial period/stage. In principle, a glacial period/stage cannot occur during a period of climatic warming, but only during a period of cooling. Using the dated ages of moraines deposited by glaciers during different periods/stages, an overall glacial chronology can be established [80]. This research compiled a glacial chronology of the EAM region. However, as this study synthesized moraine chronologies constructed using different dating techniques, chronological differences in the dated ages of the same moraine were inevitable [81–83]. For example, when analyzing the stratigraphic sedimentary sequence, OSL samples are collected from buried lateral moraine sediments, whereas ^{10}Be exposure samples are extracted from the boulders on top of the lateral moraine dams. According to the relative ages of these sediments, the OSL burial ages should be greater than the ^{10}Be exposure ages. Secondly, integral to each dating mechanism, the ^{10}Be exposure age is calculated according to the zero erosion rate, while the OSL is calculated according to the amount of cumulative exposure experienced prior to burial: this would also imply that the OSL burial age should be greater than the ^{10}Be exposure age [36]. Overall, the age of buried moraine sediments > the age of moraine exposure samples. Under the normal conditions, optically stimulated luminescence (OSL), thermoluminescence (TL), electron spin resonance (ESR) and U–series (U) dating techniques may be older than cosmogenic nuclides (^{10}Be/CRN) techniques. In addition, as glacial deposits often lack organic matter, carbon–14 (^{14}C) cannot effectively indicate age, age change may be large; potassium–argon (K–Ar) dating technique often samples volcanic sediments from the lower layer of glacial

sediments, the age may also be older. The difference of the glaciers' age cannot be avoided by different dating techniques. The effective validation of ages extracted using different dating techniques is therefore key; any chronological glacial data should be compared with the glacial history of the surrounding mountains, and chronological glacial data should be consistent with regional environmental characteristics.

The oldest extant glacial features mark the maximum local glacial extent. In other words, earlier glacial relics may have been overridden or eroded. In such cases, how can we exclude the possibility that earlier glacial advances occurred, and that the onset of any glaciation was synchronous across the study area? Mountain altitudes are a critical factor in determining the extent of any glaciation.

In western China (Figure 3), which is latitudinally adjacent to the EAM region, the oldest glaciation has been identified and named the Kunlun glacial period, which occurred during MIS 16−18 (820−620 ka) [84]. Scholars have also proposed the existence of an earlier, 1600–1700 kunlun glacial period (MIS 28−21) on the TP, otherwise known as the Hishabanma glacial period [85]. The Hengduan Mountains (HD Mts) are located on the southeastern edge of the TP. Zheng [86] recorded the earliest glacial advance in Yulong Mountain as the 600–700 Ka Yulong glacial period (MIS16–18) measured by ESR dating, which is equivalent to the late Wangkun glacial period in the TP, indicating that the HD Mts began to enter the cryosphere during this period. In the mountains of the Asia inland area (AIA), the oldest measured glacial advance was found in the remnant moraine of Gaowang Peak (Tianshan Mountain), with ESR dating results of 459.7–477.1 ka [87], corresponding to the Zhonglianggan period.

By comparing the glacial period/stage in the EAM region with those in western China, we found that there were significant differences between the extent, onset time and length of glacial periods (Figure 3). Li [14] studied the features of glaciations during the LGP in the EAM region and found that the MIS 6–5 glaciation first appeared in the coastal mountains of East Asia, indicating a strengthening glaciation. Conversely, in western China, where there were multiple glaciations, the extent of glacial ice gradually shrank. This phenomenon seems contradictory, but in fact, small East Asian coastal and island mountains only approached or reached their modern altitudes during the LGP as a result of strong neotectonic movement [88]. However, due to the uplift of the TP, the mountains in western China highly inhibited any potential climatic impact, restricting early glacial advances during the LGP. We found that the earliest records of glacial advance were in the mountains of Japan and Taiwan. Both these mountainous areas are located in an island arc that has experienced the strongest tectonic uplift, as well as major volcanic and plate activity, Taiwan and Japan are both alpine glacier types. Hebenstreit et al. [29] pointed out that the uplift rate of neotectonic movement since the LGP in the mountains of Taiwan was 5 mm/a; it has been calculated that the uplift of Mount Nanhuta since the LGM is ~275 m, potentially related to the Gonghe Movement (150 ka) [49] (Figure 3). Therefore, if monsoonal fluctuations can be taken to affect the extent of any glaciation, tectonic movement may similarly be an important determinant of the history of a glacial period/stage, it has provided an absolute spatial height basis for the development of mountain glaciers. It needs to be emphasized that tectonic movement cannot completely explain the advance and retreat of mountain glaciers, because the tectonic uplift in different are significantly different. The same monsoon circulation environment changes are the main driving force for the overall change of mountain glaciers in the study area.

5.2. Influence of EAM Circulations on Glacial Stages in the Mountains of the EAM Region during the Late Quaternary Glacial Period

Current research suggests that changes in the intensity of the EAM were caused by changes in the Earth's orbital path [89]. The EAM's principal control appears to be the degree of summer solar radiation experienced in the high latitudes of the Northern Hemisphere, as caused by precession [90,91]. The climatic evolution of the EAM therefore displays a clear Milankovitch cyclic pattern, with an orbital eccentricity of 100 ka, a plane-

tary axial tilt of 41 ka, an equinoctial precession of 23 ka, and periodic changes of 0.8 ka [92]. There is a telecorrelation between the Asian Monsoon and abrupt changes in sea surface temperatures (SSTs) and ice coverage in the North Atlantic [93]. The Early LGP in the EAM region was affected by the Greenland cold event in the North Atlantic [94], and the Heinrich event was characterized by weak monsoonal circulations [95]. The long–term evolution of the EAM is not only closely related to changes in global ice induced by solar radiation, but also to regional environmental changes such as land–sea changes, uplift of the TP, sea level fluctuations, and changes in the circulatory patterns of the Westerlies. It is a coupling process dependent upon many different factors [5]. Different climate proxies have recorded the evolution of the EAM region's environment during different periods/stages, revealing variations in monsoon intensity. By comparing these proxy archives, we found that glacier fluctuations in the EAM region are very similar to them (Figure 4). These proxies also show that climatic fluctuations within the EAM region were/are sensitive to abrupt climatic events of different scales in the Northern Hemisphere, from before the LGP (MIS 6−5), to the Early LGP (MIS 4), to the Middle LGP (MIS 3b), to the Late LGP (MIS 2/LGM–YD), and finally to the Early Holocene glacial stage (MIS 1).

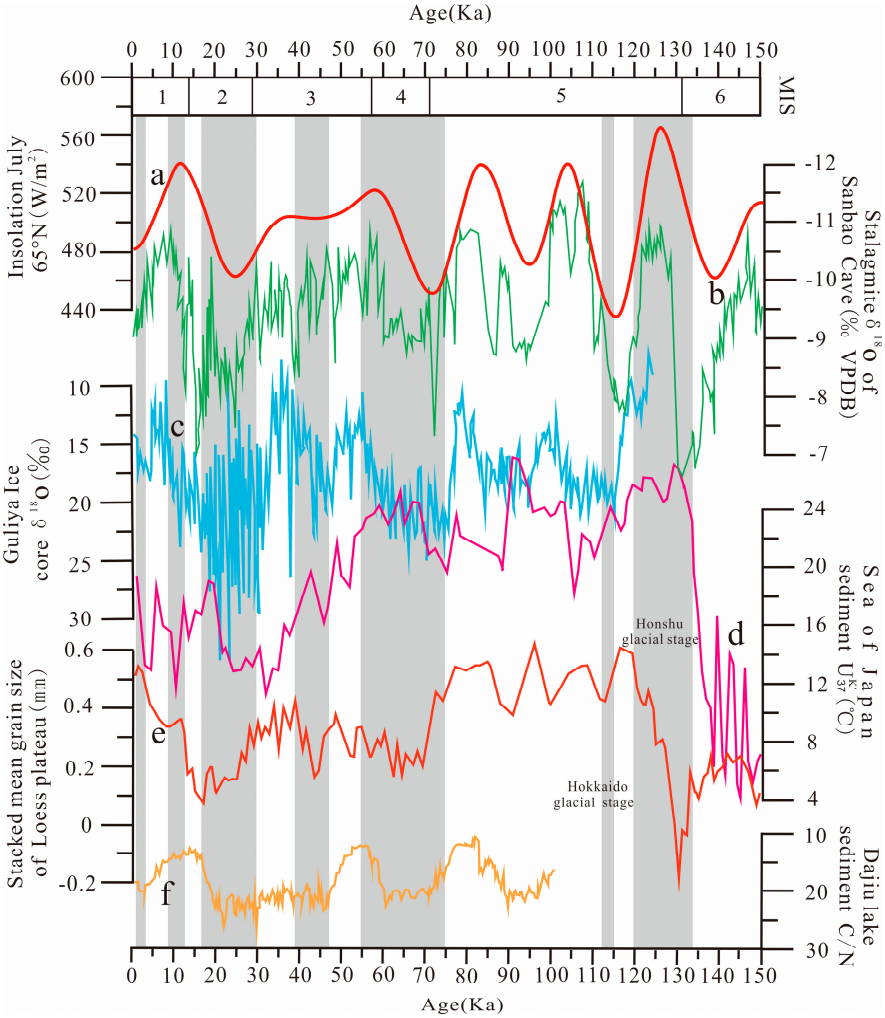


Figure 4. Comparison between glacial stages in the EAM region and the 65°N solar radiation curve, and other proxy records of the EAM. The gray lines represent the dates of mountain glaciations. (**a**) Insolation July 65 °N [96]; (**b**) Stalagmite $\delta^{18}O$ of Hulu Cave [97]; (**c**) Guliya Ice core $\delta^{18}O$ [98]; (**d**) Sea of Japan sediment UK′37 [99]; (**e**) Stacked mean grain size of Loess Plateau [100]; (**f**) Dajiu lake sediment C/N [101].

5.2.1. Penultimate Glaciation and Last Interglacial (MIS 6−5)

During the stage between MIS 6 and the LGP, the evolution of the EAM from being a principally oceanic monsoonal circulation to a continental monsoonal circulation began [102]. According to the stalagmite record extracted from Hulu Cave, monsoonal circulation patterns changed several times during this stage, with the EASM dominating [95] (Figure 5a). The amount of solar radiation changed from high to low [96], the change in the range in T values in the Sea of Japan was ~20 °C [99], and the climate was wetter than now [103]. In the EAM region, only the mountains of Japan show clear evidence of glacial advances during the Penultimate Glaciation and Last Interglacial (MIS 6–5). Although these records of glaciations in the EAM's mountainous regions remain controversial, it is nonetheless generally believed that the Late Quaternary glacial period did not begin earlier than the LGP in the EAM region [13]. However, during a period that experienced strong neotectonic movement and a moist EASM climate, we would argue that the coupling of tectonic movements, climate change and other factors might also have had a role to play in the onset of any glaciation. Conversely, as glaciation ages in different mountain ranges in the EAM region appear not entirely consistent with the glacial cycle, even after taking into account dating errors, it remains a possibility that glaciers in this region exhibited a certain lag in the recording of climate events compared with other Late Quaternary carriers, i.e., the melting and retreat time of glaciers lasted longer than any abrupt change in climate. This supposition needs to be confirmed by the collation of more chronological data and further geomorphic surveys.

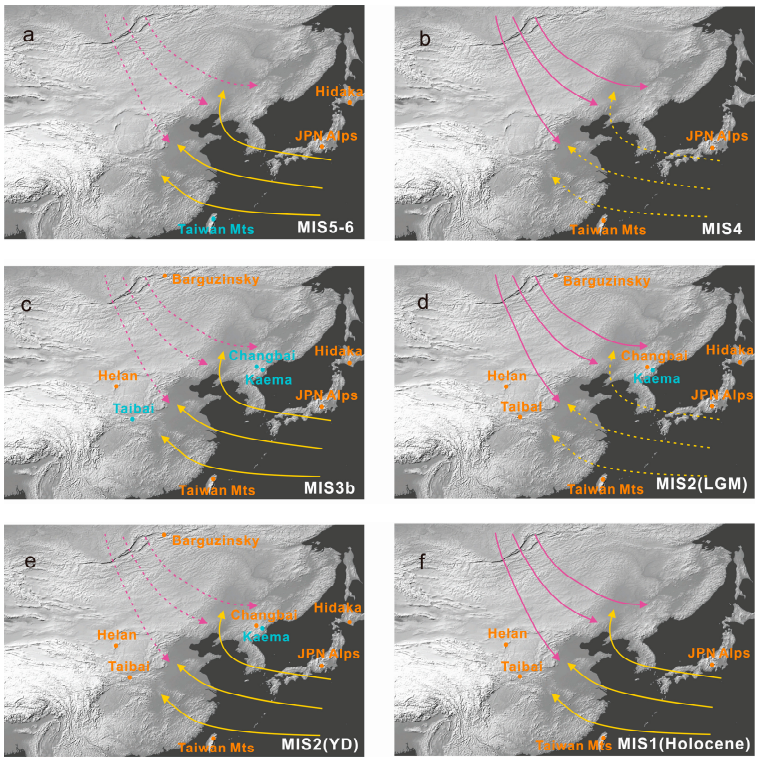


Figure 5. The responses of mountains in the EAM region to monsoonal circulations during different glacial stages. The EAWM purple and the EASM yellow, the orange words indicate the exact mountains that experienced glaciations, the blue words indicate the mountains that experienced assumed glacial advances. Purple lines represent the EAWM, yellow lines represent the EASM, dashed and solid lines indicate EAM strength. (**a**) EASM enhanced and EAWA weakened climate model MIS6−5. (**b**) EASM weakened and EAWM enhanced climate model MIS4. (**c**) EASM enhanced and EAWA weakened climate model MIS3b. (**d**) EASM weakened and EAWM enhanced climate model MIS2–LGM. (**e**) EASM enhanced and EAWM weakened climate model YD. (**f**) EAWM and EASM enhanced climate model Holocene MIS1.

5.2.2. Early LGP (MIS 4)

Studies by Japanese and Chinese scholars [53,104]. have found that in the Early LGP (MIS 4), the strong uplift of the TP forced the Westerlies to divide into southern and northern branches. The high plateau ridge of the TP caused differences in the characteristics of these northern and southern branches. The southern branch maintained a stable supply of P during the EAWM, whereas the northern branch (the Siberian–Mongolian High) became the main wind source of the EAWM [15]. After the LGP, under the control of a powerful cyclonic system, East Asia became a water vapor transport channel for monsoonal and Westerly winds [105]. Yang et al. [106] believed that the Northwest Pacific low pressure trough continued to expand and extended inland, transporting more water vapor to coastal East Asia. Although the monsoonal circulation over East Asia was weak at this time, MIS 4 also appears to have been the stage when glaciers developed the most extensively. During MIS 4, the EAWM dominated. The Guliya ice core $\delta^{18}O$ datasets show that T values were 5 °C lower than today and that P values were double modern ones [98] (Figure 5b). The remains of this glacial advance during MIS 4 are evident in the high mountains of Japan and Taiwan, reflecting the fact that, although the monsoonal circulation was weak, the cold and humid climatic environment was highly conducive to the expansion of glaciers.

5.2.3. Middle LGP (MIS3b)

Wang and Yao [107] analyzed records of the cold stage in the Middle LGP (MIS 3b) as documented in the Guliya ice core. They found that they were consistent with the solar radiation changes caused by the precession cycle of 23 ka. Although the cooling event in the Middle LGP (MIS 3b) was relatively short, there was more effective P during the Middle LGP. Climate models have suggested the existence of an enhanced EASM during MIS 3b. T was 2–4 °C higher than today, but P was 40–100% greater than modern values, meaning that there was a humid climatic environment conducive to glacial advances during this stage [108,109]; glaciers therefore became more extensive in this stage than during MIS 2 (Figure 5c). A glacial advance corresponding to MIS 3b can be traced in the Japanese Mountains, the Taiwanese Mountains and the Helan Mountains, where glacial relics are evident, and can also be inferred for Mount Taibai above 3000 m asl, where the geomorphology points to stages of glaciation.

5.2.4. Late LGP (MIS 2)

During the Late LGP (MIS 2/LGM), the cold Siberian–Mongolian High strengthened, and the T values in this region decreased sharply; at this time, the EASM was at its weakest [97]. Concurrently, the SST of the Sea of Japan dropped rapidly, the Tsushima Strait was closed, and the continental shelf was exposed [53]. Aeolian sand deposition on the Chinese Loess Plateau increased [100]. Lake biomass decreased and the C/N ratio reached a low value [101]. Hulu Cave $\delta^{18}O$ and Guliya ice core datasets have also recorded the intensity of this cooling [97,98]. A significant drop in T can therefore be assumed to have been the primary driver of glaciation during the LGM in these regions. However, there would appear to be a difference between the extent of this glaciation in the EAM region, and globally, where this stage represented the period of most significant global advance. Although the cold EAWM in this region would have been conducive to the low T values required for the development of glacial ice, a serious shortage of P probably limited the expansion of glaciers and the development of a glacial environment. During the LGM, the EAWM strengthened. The T values were 6–9 °C lower than the present day, and P was only 30–50% of what it is now [110] (Figure 5d). Conversely, because P increased, the short–lived YD cooling event in the Late LGP caused glacial advances in numerous mountain ranges in the study region [111] (Figure 5e).

5.2.5. Holocene (MIS1)

Glaciers in the EAM region began to retreat rapidly with the onset of the Early Holocene glacial stage (MIS 1), and only a few high mountains experienced a Neoglacial

glacial advance. Yi et al. [112] and Ou et al. [113] showed that the Early Holocene glacial advance in the EAM region was related to the abrupt cooling event that occurred during this stage, and that the glacial environment began to change after the onset of the dry and warm Holocene Megathermal, when the EAWM and EASM were enhanced and the Westerlies weakened [114,115]. The change in climate from winter P to summer P became established, with P becoming transitional and concentrated during the summer months, accompanied by a gradual aridification of the climate [116] (Figure 5f). The environmental deterioration after the LGM also led to the disappearance of regional glaciers in the Late Holocene. Glaciers have not been able to develop under the influence of this modern monsoonal circulation, thereby reflecting the profound impact of monsoonal fluctuations on the developmental state of mountain glaciers.

6. Conclusions

Existing chronological moraine records show that glaciations in the mountains of the EAM region only developed in a few high–altitude mountainous areas, such as the ranges of eastern China, the Taiwanese Mountains, the mountains of the Korean Peninsula, the mountains of the RFE, and the mountain ranges in the Japanese archipelago. In the EAM region, the Late Quaternary glacial period in the mountains of the East Asian archipelagos was the most complete and the longest. For example, in the mountainous areas of Japan, there were several stages of glaciation: the Penultimate Glaciation and Last Interglacial (MIS 6–5); the Early LGP (MIS 4); the Middle LGP (MIS 3b); the Late LGP (MIS 2/LGM); and the Early Holocene glacial stage (MIS 1). Taiwanese mountain glaciers developed during the Early LGP (MIS 4), the Middle LGP (MIS 3b), the Late LGP (MIS 2/LGM), and the Early Holocene glacial stage (MIS 1). Mountain glaciation sequences are shorter on the East Asian mainland, the latest glacial retreats in the EAM region (i.e., 1.7 $\pm$ 0.1 ka) occurred in the Helan Mountains; here, the glacial chronology is shorter, with glacial stages documented only for the Middle LGP (MIS 3b), the Late LGP (MIS 2/LGM), and the Early Holocene glacial stage (MIS 1). The reason for this phenomenon is that the tectonic uplift in different subregions is significantly different; on the other hand, it is also related to the difference of P between the land and sea in the monsoon climate by comparing the glacial periods in the EAM region within western China. Since 780 ka, the mountains in western China have experienced many tectonic movement events; small East Asian coastal and island mountains only approached or reached their ΔELA altitudes during the LGP as a result of strong neotectonic movement (corresponding 150 ka–Gonghe movement). We found that there were significant differences between the extent, onset time and length of glacial stages. Tectonic movement plays an important role, which reflects the particularity of the glaciations in the EAM region.

Overall, small–scale glacial advances occurred during the period before the LGP (MIS 6–5) in the EAM region in response to the EAM environment, which in turn was affected by neotectonic movement, and consequent changes to the ELA in mountainous areas. Under the constraints of monsoonal circulation patterns, glacial advances in the mountains of the EAM region gradually decreased in extent from the Early LGP (MIS 4) to the Middle LGP (MIS 3b) to the Late LGP (MIS 2/LGM–YD) and then after the LGP before completely disappearing in the Late Holocene. The time since the onset of the LGP has been affected by many periodic changes in the EAM environment. The cold–wet climate during the Early LGP was the most favorable for the development of glacial ice; abundant P promoted the development of glacial ice during the Middle LGP; however, although it was cold in the Late LGP, P decreased, and the development of glacial ice was restricted. Since the onset of the Holocene, both P and T have strengthened along a continuum. Glaciers changed gradually from a winter accumulation–summer ablation model to a summer accumulation–summer ablation model. Eventually, summer ablation exceeded summer accumulation, and the regional glacial environment deteriorated before glaciers in the EAM region disappeared completely. At present, there are no modern glaciers remaining in this region.

Author Contributions: Conceptualization, R.L. and S.Z.; methodology, L.Z. and X.W.; software, R.L.; validation, R.L. and X.W.; formal analysis, R.L.; investigation, R.L. and B.Z.; resources, C.W.; data curation, R.L. and C.W.; writing—original draft preparation, R.L.; writing—review and editing, R.L., C.W. and X.W.; supervision, L.Z.; funding acquisition, S.Z. All authors have read and agreed to the published version of the manuscript.

Funding: This research was funded by NO. U20A2082 [Key Joint Program of National Natural Science Foundation of China], NO. 41901072 and NO. 41971151 [National Natural Science Foundation of China], NO. TD2019D00 [Heilongjiang Provincial Natural Science Foundation innovation team project] and NO. HSDBSCX2022-07 [Doctoral student innovation project of Harbin Normal University].

Institutional Review Board Statement: Not applicable.

Informed Consent Statement: Not applicable.

Data Availability Statement: Some or all data used in the study are available from the corresponding author by request.

Acknowledgments: We thank two reviewers for valuable comments and suggestions that helped improve the early version of the manuscript.

Conflicts of Interest: The authors declare that there are no real or perceived conflicts of interest involved in the submission and/or publication of this manuscript.

References

1. Webster, P.J.; Magaña, V.O.; Palmer, T.N.; Shukla, J.; Tomas, R.A.; Yanai, M.; Yasunari, T. Monsoons: Processes, predictability, and the prospects for prediction. *J. Geophys. Res.* **1998**, *103*, 14451–14510. [CrossRef]
2. Lei, F.; Wei, H.Z.; Yi, S.W.; Zeng, L.; Lu, H.Y. Variations of the East Asian monsoon over the past 800 kyr constrained by the boron isotope composition of paleo–rainwater inferred from loess–paleosol deposits in NE China. Earth. *Plan. Sci. Lett.* **2021**, *561*, 116826. [CrossRef]
3. Chu, G.; Liu, J.; Schettler, G.; Li, J.; Sun, Q.; Gu, Z.; Lu, H.; Liu, Q.; Liu, T. Sediment fluxes and varve formation in Sihailongwan, a maar lake from northeastern China. *J. Paleolimnol.* **2005**, *34*, 311–324. [CrossRef]
4. Schettler, G.; Mingram, J.; Negendank, J.W.; Liu, J.Q. Palaeovariations in the East–Asian monsoon regime geo chemically recorded in varved sediments of Lake Sihailongwan (Northeast China, Jilin Province). Part 1: Hydrological conditions and dust flux. *J. Paleolimnol.* **2006**, *35*, 239–270. [CrossRef]
5. An, Z.S. The history and variability of the East Asian paleomonsoon climate. *Quat. Sci. Rev.* **2000**, *19*, 171–187. [CrossRef]
6. Xue, F.; Zhao, J.J. Intraseasonal variation of the East Asian summer monsoon in La Niña years. *Atmos. Ocean. Sci. Lett.* **2017**, *10*, 156–161. [CrossRef]
7. Li, G.Q.; Chen, F.H.; Xia, D.S.; Yang, H.; Zhang, X.J.; Madsen, D.; Oldknow, C.; Wei, H.T.; Rao, Z.G.; Qiang, M.R. A Tianshan Mountains loess–paleosol sequence indicates anti–phase climatic variations in arid central Asia and in East Asia. Earth. *Plan. Sci. Lett.* **2018**, *494*, 153–163. [CrossRef]
8. Li, J.J.; Shu, Q.; Zhou, S.Z.; Zhao, Z.J.; Zhang, J.M. Review and Prospects of Quaternary Glaciation Research in China. *J. Glaciol. Geocryol.* **2004**, *26*, 235–243.
9. Cui, Z.J.; Chen, Y.X.; Zhang, W.; Zhou, S.Z.; Zhou, L.P.; Zhang, M.; Li, C.C. Research history, glacial chronology and origins of Quaternary glaciations in China. *Quat. Sci.* **2011**, *31*, 749–764.
10. Li, J.J. Studies on the geomorphological evolution of the Qinghai–Xizang (Tibetan) Plateau and asian monsoon. *Mer. Geol. Quat. Geol.* **1999**, *19*, 1–11.
11. Shi, Y.F.; Cui, Z.J.; Li, J.J. *The Problems of Quaternary Glacier and Environment in East China*; China Science Press: Beijing, China, 1989.
12. Zhang, W.; Dong, Y.W.; Yu, Z.L.; He, M.Y. Discussion of the difference of the timing and extent of glaciers in the late Quaternary controlled by the westerly and East Asia monsoon as well as tectonic movement. *Acta Geogr. Sin.* **2013**, *68*, 909–920.
13. Zhang, W.; Liu, R.; Liu, L. Control factors on glaciation during the last glacial period in the East Asia monsoon area. *Prog. Geogr.* **2015**, *34*, 871–882.
14. Li, J.J. Glacial relics of monsoonal Asia in the last glaciation. *Quat. Sci.* **1992**, *4*, 332–339.
15. Cui, Z.J.; Zhang, W. Discussion about the glacier extent and advance/retreat asynchrony during the Last Glaciation. *J. Glaciol. Geocryol.* **2003**, *25*, 510–516.
16. Zhang, W.; Cui, Z.J.; Li, Y.H. the glacial extent and glacial advance/retreat asynchroncity in East Asia during last glaciation. *J. Geogr. Sci.* **2005**, *15*, 293–304. [CrossRef]
17. Wang, N.A.; Zhao, J.D.; Yu, Y.X.; Yu, X.R.; Zhang, W.J. The gradually improving scientific research paradigm on Quaternary glaciation in China: A review of the 4th Conference on Quaternary Glaciation and Environmental Variation in China. *J. Glaciol. Geocryol.* **2017**, *39*, 1029–1038.

18. Jing, C.R. Geomorphic characteristics of the oceanic glaier and its geoscience significance. *J. Cent. Chin. Normal Univ. Nat. Sci. Ed.* **2002**, *36*, 233–236.
19. Zhang, W.; Yan, L.; Cui, Z.J.; Yang, J.Q. Glacial environment during the Last Glacial Cycle in the mountains of East Asia. *Acta Geogr. Sin.* **2009**, *64*, 33–41.
20. BrooK, M.; Hagg, W.; WinKler, S. Contrasting medial moraine development at adjacent t emperate, maritime glaciers: Fox and Franz Josef Glaciers, South Westland, New Zealand. *Geomorphology* **2017**, *290*, 58–68. [CrossRef]
21. Pollard, D.; Kasting, J.F.; Zugger, M.E. Snowball Earth: Asynchronouscoupling of sea–glacierflow with aglobal climate model. *J. Geophys. Res.* **2017**, *122*, 5157–5171. [CrossRef]
22. Shi, Y.F. Characteristics of late Quaternary monsoon glaciation on the Tibetan Plateau and in East Asia. *Quat. Int.* **2002**, *97–98*, 79–91. [CrossRef]
23. Zhang, W.; Liu, B.B.; Cui, Z.J.; Li, Y.Y.; Liu, L. Theoretical glacial equilibrium line altitudes and their influencing factors in the typical mountains of China. *Acta Geogr. Sin.* **2014**, *69*, 958–968.
24. Su, B.; Li, Z.Q.; Zhang, M.J.; Guo, R.; Sun, M.P.; Che, Y.J.; Ying, X. A comparative study on mass balance betw een the continental glaciers and the temperate glaciers: Taking the typical glaciers in the Tianshan Mountains and the Alps as examples. *J. Glaciol. Geocryol.* **2015**, *37*, 1131–1140.
25. Gen, K.; Yang, Z.R. Climatic characteristics and climatic landforms in Helan Mountain. *Yantai Normal College. J.* **1990**, *6*, 49–56.
26. Zhang, W.; Liu, L.; Chen, Y.X.; Liu, B.B.; Harbor, J.M.; Cui, Z.J.; Liu, R.; Liu, X.; Zhao, X. Late glacial ^{10}Be ages for glacial landforms in the upper region of the Taibai glaciation in the Qinling Mountain range, China. *J. Asian Earth Sci.* **2016**, *115*, 383–392. [CrossRef]
27. Zhang, C.Z.; Nan, W.Z.; Tai, S.H.; Li, Z.J. Analysis of meterological conditions of Tianchi in Changbai Mountain. *J. Yanbian Univ. Agric. Sci. Ed.* **2007**, *29*, 33–36.
28. Jin, Z.; Ni, X. Climatology of Hail in North Korea. *J. Pekinensis Univ. Nat. Sci. Ed.* **2015**, *51*, 437–443.
29. Hebenstrieit, R.; Böse, M.; Murray, A. Late Pleistocene and early Holocene glaciations in Taiwanese mountains. *Quat. Int.* **2006**, *147*, 76–88. [CrossRef]
30. Mokhova, L.; Tarasov, P.; Bazarova, V.; Klimin, M. Quantitative biome reconstruction using modern and late Quaternary pollen data from the southern part of the Russian Far East. *Quat. Sci. Rev.* **2009**, *28*, 2913–2926. [CrossRef]
31. Igarashi, Y.; Igarashi, T.; Endo, K.; Yamada, O.; Nakagava, M.; Sumita, M. Vegetation history since the Late Glacial of Habomai Bog and Ochiishi Cape Bog, Nemuro Peninsula, eastern Hokkaido, north Japan, Japan. *J. Hist. Bot.* **2001**, *10*, 67–79.
32. Nakagawa, T.; Tarasov, P.E.; Nishida, K.; Gotanda, K.; Yasuda, Y. Quantitative pollen–based climate reconstruction in central Japan: Application to surface and Late Quaternary spectra. *Quat. Sci. Rev.* **2002**, *21*, 2099–2113. [CrossRef]
33. Zhang, W.; He, M.Y.; Li, Y.H.; Cui, Z.J.; Wang, Z.L.; Yu, Y. Quaternary glacier development and the relationship between the climate change and tectonic uplift in the Helan Mountain. *Chin. Sci. Bull.* **2012**, *57*, 4491–4504. [CrossRef]
34. Rost, K.T. Paleoclimatic field studies in and along the Qinling–shan (Central China). *Geojournal* **1994**, *34*, 107–120. [CrossRef]
35. Gu, J.N. Quaternary Glacial Geomorphology and Glacial Deposits Features of the Taibai Mountain, Qinling Mountains. Master's Thesis, China University of Geosciences, Beijing, China, 2017.
36. Liu, L.; Zhang, H.J.; Zhang, W.; Chai, L. Global Last Glacial Maximum climate inferred from reconstructing the Eryehai Valley, Mount Taibai, Qinling Mountains, eastern China. *Palaeogeogr. Palaeoclimatol. Palaeoecol.* **2022**, *590*, 110858. [CrossRef]
37. Zhang, W.; Niu, Y.B.; Yan, L.; Cui, Z.J.; Li, C.C. Late Pleistocene glaciations of Changbai Mountains in northeastern China. *Chin. Sci. Bull.* **2008**, *53*, 2672–2684. [CrossRef]
38. Hebenstreit, R.; Böse, M. Geomorphological evidence for a Late Pleistocene glaciation in the high mountains of Taiwan dated with age estimates by optically stimulated luminescence (OSL). *Z. Geomorphol. Suppl.* **2003**, *130*, 31–49. [CrossRef]
39. Cui, Z.J.; Yang, C.F.; Liu, G.N.; Zhang, W.; Wang, S.; Sung, Q.C. The Quaternary glaciation of Shesan Mountain in Taiwan and glacial classification in monsoon areas. *Quat. Int.* **2002**, *97–98*, 147–153. [CrossRef]
40. Hebenstreit, R.; Ivy–Ochs, S.; Kubik, P.W.; Schlüchter, C.; Böse, M. Lateglacial and early Holocene surface exposure ages of glacial boulders in the Taiwanese high mountain range. *Quat. Sci. Rev.* **2011**, *30*, 298–311. [CrossRef]
41. Siame, L.; Chu, H.T.; Carcaillet, J.; Bourles, D.; Braucher, R.; Lu, W.C.; Angelier, J.; Dussouliez, P. Glacial retreat history of Nanhuda Shan from preserved glacial features: The cosmic ray exposure perspective. *Quat. Sci. Rev.* **2007**, *26*, 2185–2200. [CrossRef]
42. Osipov, E.Y. Equilibrium–line altitudes on reconstructed LGM glaciers of the northwest Barguzinsky Ridge, Northern Baikal, Russia. *Palaeogeogr. Palaeoclimatol. Palaeoecol.* **2004**, *209*, 219–226. [CrossRef]
43. Yanagida, M. Age of the Shikotsu pumice fall–1 deposit. *Quat. Res.* **1994**, *33*, 205–207. [CrossRef]
44. Machida, H.; Arai, F. *Atlas of Tephra in and Around Japan*; University of Tokyo Press: Tokyo, Japan, 2004.
45. Kondoa, R.; Tsukamoto, S.; Tachibanaa, H.; Miyairi, Y.; Yokoyama, Y. Age of glacial and periglacial landforms in northern Hokkaido, Japan, using OSL dating of fine grain quartz. *Quat. Geochronol.* **2007**, *2*, 260–265. [CrossRef]
46. Ono, Y. Glacial and Periglacial Paleoenvironments in the Japanese Islands. *Quat. Res.* **1991**, *30*, 203–211. [CrossRef]
47. Aoki, T. Younger Dryas glacial advances in Japan dated with in situ produced cosmogenic radionuclides, Transactions. *Jpn. Geochronol. Union.* **2003**, *24*, 27–39.
48. Aoki, T. Chronological Study of Glacial Advances Based on the Weathering–Rind Thickness of Morainic Gravels in the Northern Part of the Central Japan Alps. *Geogr. Rev. Jpn.* **1994**, *67*, 601–618. [CrossRef]
49. Kawasumi, T. Ages of Glaciations in the Early Stage of the Late Pleistocene, Based on Glacial and Volcanic Deposits in Tateyama, Hida Mountains, Central Japan. *Geogr. Rev. Jpn.* **2000**, *73A*, 26–43. [CrossRef]

50. Ono, Y.; Aoki, T.; Hasengawa, H.; Liu, D. Mountain glaciation in Japan and Taiwan at the global Last Glacial Maximum. *Quat. Int.* **2005**, *138–139*, 79–92. [CrossRef]
51. Nanzawa, K.; Hirakawa, K. Glaciation and Accumulation Terracing in the Yabusawa Valley, Mt. Senjogatake in the Southern Japanese Alps, since the Last Glacial Stage. *Geogr. Rev. Jpn.* **2000**, *73A–2*, 124–136.
52. Ehlers, J.; Gibbard, P.L. *Quaternary Glaciations Extent and Chronology*; Elsevier Press: Amsterdam, The Netherlands, 2011.
53. Ono, Y.; Naruse, T. Snowline elevation and eolian dust flux in the Japanese islands during isotope stages 2 and 4. *Quat. Int.* **1997**, *37*, 45–54. [CrossRef]
54. Ono, Y. Last glacial paleoclimate reconstructed from glacial and periglacial landforms in Japan. *Geogr. Rev.* **1984**, *57B*, 87–100. [CrossRef]
55. Tian, Z.S. A study about the traces of Quaternary glaciation of Mount Taibai in Shanxi province. *J. Northwest Univ. Nat. Sci. Ed.* **1981**, *22*, 59–69.
56. Ma, Q.H.; He, Y.Q. Moraine Features end Ice Ages of the Quaternary in the Taibai Mountain. *J. Glaciol. Geocryol.* **1988**, *10*, 66–75.
57. Kano, T. Contribution to the glacial topography of Tunifak Mountain Formosa. *Geogr. Rev. Jpn.* **1935**, *11*, 242–243. [CrossRef]
58. He, L.D.; Chen, S.H. Taiwan's Quaternary Mountain Glacier Retreat Models. *J. Geogr. Sci.* **2010**, *59*, 19–38.
59. He, L.D.; Liu, R.H. The Relationships between Weathered Rock Surface Hardness and Exposure Dates of Quaternary Erratic Boulders in Nanhudashan of Taiwan. *J. Geogr. Sci.* **2012**, *67*, 31–47.
60. Song, C.Q.; Zhao, C.N. The discovery its significance of Quaternary glacial relics in Taiwan. *Prog. Geogr.* **1999**, *18*, 95–96.
61. Zhu, C.; Qi, S.Z.; He, L.D.; Zhang, W.; Jiang, X.F.; Wu, L. Investigation and Analysis of Quaternary Glacier Geomorphology in Mt.Jade, Taiwans Highest Peak, China. *J. Anhui Normal Univ. Nat. Sci. Ed.* **2019**, *42*, 414–419.
62. Kano, T. Preliminary notes on the morphology of the High Mountain Lands of Formosa. *Geogr. Rev. Jpn.* **1932**, *8*, 196–202. [CrossRef]
63. Zhang, W.; Cui, Z.J.; Yan, L. Present and late Pleistocene equilibrium line altitudes in Changbai Shan, Northeast China. *J. Geogr. Sci.* **2009**, *19*, 373–383. [CrossRef]
64. Astakhov, V. Middle Pleistocene glaciations of the Russian North. *Quat. Sci. Rev.* **2004**, *23*, 1285–1311. [CrossRef]
65. Gillespie, A.; Molnar, P. Asynchronous maximum advances of mountain and continental glaciers. *Rev. Geophys. Sci.* **1995**, *33*, 311–364. [CrossRef]
66. Brigham–Grette, J.; Gualtieri, L.M.; Glushkova, O.Y.; Hamilton, T.D.; Mostoller, D.; Kotov, A. Chlorine–36 and ^{14}C chronology support a limited last glacial maximum across central Chukotka, northeastern Siberia, and no Beringian ice sheet. *Quat. Res.* **2003**, *59*, 386–398. [CrossRef]
67. Svendsen, J.I.; Alexanderson, H.; Astakhov, V.I.; Demidov, I.; Dowdeswell, J.A.; Funder, S.; Gataullin, V.; Henriksen, M.; Hjort, C.; Houmark–Nielsen, M.; et al. Late Quaternary ice sheet history of northern Eurasia. *Quat. Sci. Rev.* **2004**, *23*, 1229–1271. [CrossRef]
68. Arkhipov, S.A.; Isayeva, L.L.; Bespaly, V.G.; Glushkova, O. Glaciation of Siberia and North–East USSR. *Quat. Sci. Rev.* **1986**, *5*, 463–474. [CrossRef]
69. Stauch, G.; Lehmkuhl, F.; Frechen, M. Luminescence chronology from the Verkhoyansk Mountains (North–Eastern Siberia). *Quat. Geochronol.* **2007**, *2*, 255–259. [CrossRef]
70. Hashimoto, S.; Kumano, S. Zur Gletschert opographie im Hidaka—Gebirge, Hokkaido, Japan (Uebersicht). *Geogr. Rev. Jpn.* **1955**, *61*, 208–217.
71. Iwasaki, S.; Hirakawa, K.; Sawagaki, T. Late Quaternary Glaciation in the Esaoman–Tottabetsu Valley, Hidaka Range, Hokkaido. *Jpn. J. Geogr.* **2000**, *109*, 37–55. [CrossRef]
72. Osada, T. Two arguments about glaciers in Japan. *Assoc. Geol. Collab. Jpn.* **2011**, *66*, 80–87.
73. Aoki, T. Classification and characteristics of the distribution of glacial landforms in the Japanese Alps. *J. Geophys.* **2002**, *111*, 498–508.
74. Kawasumi, T. Timing of Glacial Advances and Volcanic Activities on Mt. Tateyama, Hida Range, Central Japan during the Late Stade of the Last Glacial Period. *Quat. Res.* **2007**, *46*, 37–46. [CrossRef]
75. Hasegawa, H. Glacial and Periglacial Landforms around Mt. Kasaga–take, Northern Japanese Alps. *Geogr. Rev. Jpn.* **1996**, *69*, 75–101. [CrossRef] [PubMed]
76. Aoki, T. Chronometry of the glacial deposits based on the ^{10}Be exposure age method case study in Senjojiki cirque and Nogaike cirque, northern part of the Kiso mountain range. *Quat. Res.* **2000**, *39*, 189–198. [CrossRef]
77. Kind, N.V. Late Quaternary climatic changes and glacial events in the Old and New World radiocarbon chronology. *Int. Geol. Cong. Montreal. Sect.* **1972**, *12*, 55–61.
78. Zhang, W.; Chai, L.; Ians, E.; Liu, L.; Li, Y.P.; Qiao, J.R.; Tang, Q.Y.; Sun, B. Geomorphic features of Quaternary glaciation in the Taniantaweng Mountain, on the southeastern Qinghai–Tibet Plateau. *J. Mt. Sci.* **2019**, *16*, 256–274. [CrossRef]
79. Lisiecki, L.E.; Raymo, M.E. A Pliocene–Pleistocene stack of 57 globally distributed benthic δ^{18}O records. *Paleoceanogr.* **2005**, *20*, 1–17. [CrossRef]
80. Chevalier, M.L.; Hilley, G.; Tapponnier, P.; Woerd, J.V.D.; Zeng, J.L.; Finkel, R.C. Constraints on the late Quaternary glaciations in Tibet from cosmogenic exposure ages of moraine surfaces. *Quat. Sci. Rev.* **2011**, *30*, 528–554. [CrossRef]
81. Xu, X.K.; Yang, J.Q.; Dong, G.C.; Wang, L.Q.; Miller, L. OSL dating of glacier extent during the Last Glacial and the Kanas Lake basin formation in Kanas River valley. *Geomorphology* **2009**, *112*, 306–317. [CrossRef]

82. Ou, X.J.; Lai, Z.P.; Zhou, S.Z.; Zeng, L.H. Timing of glacier fluctuations and trigger mechanisms in eastern Qinghai–Tibetan Plateau during the late Quaternary. *Quat. Res.* **2014**, *81*, 464–475. [CrossRef]
83. Chen, A.D.; Tian, M.Z.; Zhou, Z.Z. Macroscopic and microscopic evidence of Quaternary glacial features and ESR dating in the Daweishan Mountain area, Hunan, eastern China. *Quat. Int.* **2014**, *333*, 62–68. [CrossRef]
84. Owen, L.A.; Finkel, R.C.; Barnard, P.L.; Haizhou, M.; Asahi, K.; Caffee, M.W.; Derbyshire, E. Climatic and topographic controls on the style and timing of late Quaternary glaciation throughout Tibet and the Himalaya defined by ^{10}Be cosmogenic radionuclide surface exposure dating. *Quat. Sci. Rev.* **2005**, *24*, 1391–1411. [CrossRef]
85. Zheng, B.X.; Xu, Q.; Shen, Y. The relationship between climate change and Quaternary glacial cycles on the Qinghai–Tibetan Plateau: Review and speculation. *Quat. Int.* **2002**, *97*, 93–101. [CrossRef]
86. Zheng, B.X. Quaternary glaciation and glacier evolution in the Yulong Mount, Yunnan. *J. Glaciol. Geocryol.* **2000**, *22*, 53–61.
87. Zhao, J.D.; Zhou, S.Z.; He, Y.Q.; Ye, Y.G.; Liu, S.Y. ESR dating of glacial tills and glaciations in the Urumqi River headwaters, Tianshan Mountains, China. *Quat. Int.* **2006**, *144*, 61–67. [CrossRef]
88. Ehlers, J.; Gibbard, P.L. The extent and chronology of Cenozoic Global Glaciation. *Quat. Int.* **2007**, *164–165*, 6–10. [CrossRef]
89. Yi, L.; Shi, Z.G.; Tan, L.C.; Deng, C.L. Orbital scale nonlinear response of East Asian summer monsoon to its potential driving forces in the late Quaternary. *Clim. Dynam.* **2018**, *6*, 2183–2197. [CrossRef]
90. Prell, W.L.; Kutzbach, J.E. Monsoon variability over the past 150,000 years. *J. Geophys. Res.* **1987**, *92*, 8411–8425. [CrossRef]
91. Ding, Z.L.; Liu, T.S.; Rutter, N.W.; Yu, Z.; Zhu, R. Lce–volume forcing of East Asian winter monsoon variations in the past 800,000 years. *Quat. Res.* **1995**, *44*, 149–159. [CrossRef]
92. Kukla, G.; An, Z.S.; Melice, J.L.; Gavin, J.; Xiao, J.L. Magnetic susceptibility record of Chinese loess. *Earth. Environ. Sci. Trans. R. Soc. Edinb.* **1990**, *81*, 263–288. [CrossRef]
93. Li, N.N.; Sharifi, A.; Chambers, F.M.; Ge, Y.; Dubois, N.; Gao, G.Z.; Li, D.H.; Liu, L.D.; Liu, H.Y.; Wang, J.Y.; et al. Linking Holocene East Asian monsoon variability to solar forcing and ENSO activity: Multi–proxy evidence from a peatland in Northeastern China. *Holocene* **2021**, *31*, 966–982. [CrossRef]
94. Yang, S.L.; Dong, X.X.; Xiao, J.L. The East Asian Monsoon since the Last Glacial Maximum: Evidence from geological records in northern China. Sci. Chin. *Earth. Sci.* **2019**, *62*, 1181–1192. [CrossRef]
95. Marzin, C.; Kallel, N.; Kageyama, M.; Duplessy, J.C.; Braconnot, P. Glacial fluctuations of the Indian monsoon and their relationship with North Atlantic climate: New data and modelling experiments. *Clim. Past.* **2013**, *9*, 2135–2151. [CrossRef]
96. Berger, A. Long–Term Variations of Caloric Insolation Resulting from the Earth's Orbital Elements. *Quat. Res.* **1978**, *9*, 139–167. [CrossRef]
97. Wang, Y.J.; Cheng, H.; Edwards, R.L.; An, Z.S.; Wu, J.Y.; Shen, C.C.; Dorale, A.J. A high resolution absolute dated late pleistocene monsoon record from Hulu Cave, China. *Science* **2001**, *294*, 2345–2348. [CrossRef] [PubMed]
98. Thompson, L.G.; Yao, T.D.; Davis, M.E.; Henderson, K.A.; Mosley–Thompson, E.; Lin, P.N.; Beer, J.; Synal, H.A.; Cole–Dai, J.; Bolzan, J.F. Tropical climate instability: The last glacial cycle from a Qinghai–Tibetan ice core. *Science* **1997**, *276*, 1821–1825. [CrossRef]
99. Liu, Y.G.; Chen, J.J.; Chen, J.X.; Xing, L.; Zou, J.J.; Yao, Z.Q. Variations of alkenone temperature in the Sea of Japan during the last 170 ka and its paleoceanographic implications. *Chin. Sci. Bull.* **2014**, *59*, 4498–4509. [CrossRef]
100. Sun, Y.; Chen, J.; Clemens, S.; Liu, Q.; Ji, J.; Tada, R. East Asian monsoon variability over the last seven glacial cycles recorded by a loess sequence from the northwestern Chinese Loess Plateau. *Geochem. Geophys. Geosyst.* **2006**, *7*, Q12Q02. [CrossRef]
101. Pan, J.J.; Huang, H.J.; Zhang, R.; Huang, C.J.; Liu, J.S. The variation of carbon and nitrogen isotopic compositions in the Dajiuhu sediments and climate changes since Late Pleistocene in the western Hubei of Central China. *Quat. Sci.* **2021**, *41*, 916–930.
102. Yuan, D.X.; Cheng, H.; Edwards, R.L.; Dykoski, C.A.; Kelly, M.J.; Zhang, M.L.; Qing, J.M.; Lin, Y.S.; Wang, Y.J.; Wu, J.Y.; et al. Timing, duration, and transitions of the Last Interglacial Asian monsoon. *Science* **2004**, *304*, 575–578. [CrossRef]
103. Chen, F.H.; Xu, Q.H.; Chen, J.H.; Birks, H.J.B.; Liu, J.B.; Zhang, S.R.; Jin, L.Y.; An, C.B.; Telford, R.J.; Cao, X.Y.; et al. East Asian summer monsoon precipitation variability since the last deglaciation. *Sci. Rep.* **2015**, *5*, 11186. [CrossRef]
104. Zhang, W.; Cui, Z.J.; Li, Y.H. Review of the timing and extent of glaciers during the last glacial cycle in the bordering mountains of Tibet and in East Asia. *Quat. Int.* **2006**, *154–155*, 32–43. [CrossRef]
105. Chen, F.H.; Chen, J.H.; Huang, W.; Chen, S.Q.; Huang, X.Y.; Jin, L.Y.; Jia, J.; Zhang, X.J.; An, C.B.; Zhang, J.W.; et al. Westerlies Asia and monsoonal Asia: Spatiotemporal differences in climate change and possible mechanisms on decadal to sub–orbital timescales. *Earth. Sci. Rev.* **2019**, *192*, 337–354. [CrossRef]
106. Yang, S.; Lau, K.T.; Kim, K.M. Variations of the East Asian jet stream and Asian–Pacific–American winter climate anomalies. *J. Climate.* **2002**, *15*, 306–325. [CrossRef]
107. Wang, Y.Q.; Yao, T.D. Progresses in the Studies of Abrupt Climatic Change Events Recorded inIce Cores During the Last Glacial–Interglacial Cycle. *J. Glaciol. Geocryol.* **2002**, *24*, 550–558.
108. Cui, Z.J.; Yang, J.F.; Liu, G.N.; Song, G.C.; Wang, X. Monsoon Development and Glacier Disappearance–From the point of view of glacier revolution features during last glaciation in Xueshan, Taiwan. *J. Glaciol. Geocryol.* **2000**, *3*, 7–13.
109. Shi, Y.F.; Liu, X.; Li, B.; Yao, T. A very strong summer monsoon event during 30–40 ka BP in the Qinghai–Xizang (Tibet) plateau and its relation to precessional cycle. *Chin. Sci. Bull.* **1999**, *44*, 1851–1857. [CrossRef]
110. Ono, Y.; Shulmeister, J.; Lehmkuhl, F.; Asahi, K.; Aoki, T. Timing and causes of glacial advances across the PEP–II Transect (East–Asia to Antarctica) during the last glaciation cycle. *Quat. Int.* **2004**, *118–119*, 55–68. [CrossRef]

111. Shi, Y.F.; Cui, Z.J.; Su, Z. *Quaternary Glaciations and Environmental Variations in China*; Hebei Science and Publishing House Press: Shijiazhuang, China, 2006.
112. Yi, C.L.; Chen, H.L.; Yang, J.Q.; Liu, B.; Fu, P.; Liu, K.X.; Li, S. Review of Holocene glacial chronologies based on radiocarbon dating in Tibet and its surrounding mountains. *J. Quat. Sci.* **2008**, *23*, 533–543. [CrossRef]
113. Ou, X.J.; Lai, Z.P.; Zeng, L.H.; Zhou, S.Z. OSL dating of glacial sediments from the Qinghai–Tibetan Plateau and its bordering mountains: A review and methodological suggestions. *Carpath. J. Earth. Environ.* **2012**, *3*, 743–756. [CrossRef]
114. Bazarova, V.B.; Klimin, M.A.; Mokhova, L.M.; Orlova, L.A. New pollen records of Late Pleistocene and Holocene changes of environment and climate in the Lower Amur River basin, NE Eurasia. *Quat. Int.* **2008**, *179*, 9–19. [CrossRef]
115. Zhou, W.J.; Zheng, Y.H.; Meyers, P.A.; Jull, A.T.; Xie, S.C. Postglacial climate–change record in biomarker lipid compositions of the Hani peat sequence, Northeastern China. *Earth. Plan. Sci. Lett.* **2010**, *295*, 37–46. [CrossRef]
116. Gotanda, K.; Nakagawa, T.; Tarasov, P.; Kitagawa, J.; Inoue, Y.; Yasuda, T. Biome classifification from Japanese pollen data: Application to modern–day and Late Quaternary samples. *Quat. Sci. Rev.* **2002**, *21*, 647–657. [CrossRef]

Disclaimer/Publisher's Note: The statements, opinions and data contained in all publications are solely those of the individual author(s) and contributor(s) and not of MDPI and/or the editor(s). MDPI and/or the editor(s) disclaim responsibility for any injury to people or property resulting from any ideas, methods, instructions or products referred to in the content.